J Appl Electrochem (2010) 40:2171–2183
DOI 10.1007/s10800-010-0199-2

ORIGINAL PAPER

An experimental and theoretical investigation of adsorption characteristics of a Schiff base compound as corrosion inhibitor at mild steel/hydrochloric acid interface

I. Ahamad · C. Gupta · R. Prasad · M. A. Quraishi

Received: 16 January 2010 / Accepted: 5 September 2010 / Published online: 19 September 2010

Abstract This study investigates the effect of a Schiff base namely 2-[2-(2-(3-phenylallylidene)hydrazine carbonothioyl)hydrazinecarbonyl]benzoic acid (SB), on corrosion inhibition of mild steel in 1 M HCl. Electrochemical impedance measurement, potentiodynamic polarization and weight loss methods were applied to study adsorption of SB at metal/solution interface. Results revealed that SB is an excellent inhibitor for mild steel corrosion in 1 M HCl; showing a maximum efficiency 99.5% at concentration of 1.36×10^{-6} M. Fourier transform infrared spectroscopy (FTIR) observations of the mild steel surface confirmed the formation of protective film on the metal surface by studied compound. Polarization studies showed that SB is a mixed-type inhibitor. Adsorption process obeyed Langmuir's model with a standard free energy of adsorption (ΔG°_{ads}) of -46.7 kJ mol^{-1}. Energy gaps for interactions between mild steel surface and inhibitor were found to be close to each other showing that SB possess capacity to behave as both electron donor and acceptor.

Keywords Corrosion inhibition · Schiff base · FTIR · Electrochemical measurement · Adsorption · Quantum chemical calculation

I. Ahamad · M. A. Quraishi (✉)
Department of Applied Chemistry, Institute of Technology, Banaras Hindu University, Varanasi 221 005, India
e-mail: maquraishi@rediffmail.com; maquraishi.apc@itbhu.ac.in

R. Prasad
Department of Chemistry, Faculty of Science, Banaras Hindu University, Varanasi 221 005, India

C. Gupta
Department of Chemistry, Kutir P.G. College, Chakke, Jaunpur 222 146, India

1 Introduction

The use of inhibitors to control the destructive attack of acid environment has found widespread applications in many industrial processes such as acid cleaning, acid pickling, acid descaling, and oil well acidizing [1]. The applicability of organic compounds as corrosion inhibitors for metals in acidic media has been recognized for a long time [2–4]. Most of the effective organic inhibitors used contain heteroatoms such as O, N, S and multiple bonds in their molecules through which they are adsorbed on the metal surface [5–8]. It has been observed that adsorption depends mainly on certain physico-chemical properties of the inhibitor group, such as functional groups, electron density at the donor atom, π-orbital character, and the electronic structure of the molecule [9].

For proper selection of inhibitors, chemical and electrochemical techniques coupled with surface analytical techniques can be used for characterization of inhibitors but a need exists for a systematic approach for characterization of the interaction between the organic inhibitor molecules and the metal surfaces in order to search new and efficient corrosion inhibitors. More recent studies have shown that the inhibitive effect for steel in acid solutions can be enhanced by increasing the number of hetero-atoms in organic compounds. Schiff bases have been investigated for their corrosion inhibition effect on various metals and alloys in acid media [10–14]. Schiff bases are the condensation products of an amine and a ketone or aldehyde. The inhibition efficiency of Schiff bases is much more than that of the corresponding amines and aldehyde because Schiff bases ($R_2C{=}NR$) have both the features (heteroatoms and π electrons) combined with their structure. Pi (π) electrons in the Schiff base molecule not only can locate the unoccupied orbital of the transition metal, but also can

accept the electrons of the d orbital of the transition metal to form feed back metal–inhibitor bond, which is not possible with an amine. Based on the presence of nitrogen atoms and the imine functional group in its structure, Schiff base molecule may reasonably justify its use as an effective corrosion inhibitor [15].

The quantum-chemical calculations have been widely used to study the reaction mechanisms and to interpret the experimental results as well as to solve chemical ambiguities. This is a useful approach to investigate the mechanisms of reaction in the molecule and its electronic structure level and electronic parameters can be obtained by means of theoretical calculations using the computational methodologies of quantum chemistry [16]. The advancement in methodology and implementations has reached a point where predicted properties of reasonable accuracy can be obtained from density functional theory (DFT) calculations [17]. The geometry of the inhibitor in its ground state, as well as the nature of their molecular orbitals, highest occupied molecular orbital (HOMO) and lowest unoccupied molecular orbital (LUMO) are involved in the properties of activity of inhibitors. The inhibition property of a compound has been often correlated with energy of HOMO, LUMO and HOMO–LUMO gap. However, we found that it is fundamentally more appropriate to correlate inhibition property with vertical ionization potential (*IP*), vertical electron affinity (*EA*) and molecular band gap (ΔE_{MBG}). Therefore, it is worth to compute these properties theoretically.

The present contribution aims to investigate the adsorption characteristics and inhibition properties of a Schiff base compound namely, 2-[2-(2-(3-phenylallylidene)hydrazinecarbonothioyl)hydrazine carbonyl]benzoic acid (SB) at mild steel/hydrochloric acid interface using weight loss, electrochemical impedance, polarization techniques and quantum chemical calculations. This SB was synthesized conveniently by condensation of phthallic anhydride, TCH and cinnamaldehyde in high yield. This compound contained more hetero-atoms and phenylallylic moiety in conjugation with azomethine (C=N) group. Further SB molecule is big enough to block large surface area of the metal. In view of these favorable features the SB was synthesized for the present work. Adsorbed film of inhibitor at metal/solution interface has been confirmed using reflectance Fourier transform infrared spectroscopy (FTIR) technique.

2 Experimental

Schiff base compound (SB) was synthesized by condensation reaction of precursor compound IL_1 with cinnamaldehyde. The precursor compound IL_1 itself was synthesized from reaction of phthalic anhydride with thiocarbohydrazide (TCH) according to the procedure described in literature [18]. The percentage yield, melting point and R_f value of the synthesized SB were 91%, 208–209 °C and 0.41 respectively. Important IR peaks are: 1290 cm^{-1} (C=S str), 1384, 1544 cm^{-1} (C=C str (aromatic rings)), 1625 cm^{-1} (C=N str), 1727 cm^{-1} (C=O str), 2603 cm^{-1} (O–H str (COOH)), 2983 cm^{-1} (Ar–H str), and 3447 cm^{-1} (N–H str). The synthetic root, IUPAC name and structure of SB is given in Scheme 1. All the chemicals chosen for our study were of analytical grade and double distilled water was used throughout the experiment. Further, the inhibitor solution was prepared in water:ethanol mixture (10:1 ratio) to ensure the solubility.

Prior to all measurements, the mild steel specimens, having composition (in wt%) 0.076 C, 0.012 P, 0.026 Si, 0.192 Mn, 0.050 Cr, 0.135 Cu, 0.023 Al, 0.050 Ni and the remainder iron, were abraded successively with fine grade

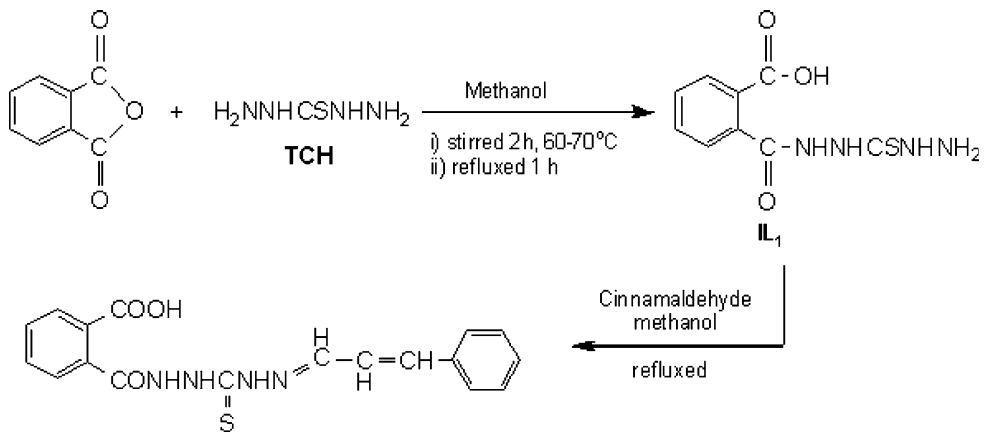

Scheme 1 Synthetic root, chemical structure and IUPAC name of 2-[2-(2-(3-phenylallylidene)hydrazinecarbonothioyl)hydrazine carbonyl]benzoic acid (SB)

emery papers (600–1200 grade). The specimens were washed thoroughly with double distilled water and finally degreased with acetone and dried at room temperature. The aggressive solution 1 M HCl was prepared by dilution of analytical grade HCl (37%) with double distilled water and all experiments were carried out in unstirred solutions.

Electrochemical impedance measurements (EIS) and potentiodynamic polarization studies were carried out using a GAMRY PCI 4/300 electrochemical work station based on ESA 400. Gamry applications include EIS 300 (for EIS measurements) and DC 105 software for corrosion and Echem Analyst 5.50 software for data fitting. All electrochemical experiments were performed in a Gamry three electrodes electrochemical cell under atmospheric condition with a platinum counter electrode and a saturated calomel electrode (SCE) as the reference electrode. The working electrode mild steel (7.5 cm long stem) with the exposed surface of 1.0 cm^2, was immersed into aggressive solutions with and without inhibitor, and then the open circuit potential was measured after 30 min. EIS measurements were performed at corrosion potentials, E_{corr}, over a frequency range of 100 kHz to 10 mHz with an AC signal amplitude perturbation of 10 mV peak to peak. Potentiodynamic polarization studies were performed with a scan rate of 1 mVs^{-1} in the potential range from 250 mV below the corrosion potential to 250 mV above the corrosion potential. All potentials were recorded with respect to the SCE.

Weight loss measurements were performed on the mild steel specimens of size 2.5 cm × 2.0 cm × 0.25 cm in 1 M HCl solution with and without addition of different concentrations of inhibitor [19]. Every sample was weighed by an electronic balance and then placed in the aggressive solution. The duration of the immersion was 3 h at the temperature range from 308 to 338 (±0.5) K. Effect of immersion times on protective film/or layer at metal/solution interface was carried out at 308 K for a time range 3–24 h. After immersion, the surface of the specimen was cleaned by double distilled water followed by rinsing with acetone and the specimens were weighed again in order to calculate inhibition efficiency and corrosion rate. The experiments were done in triplicate and the average value of the weight loss was noted. For each experiment, a freshly prepared solution was used and the solution temperature was thermostatically controlled at a desired value.

FTIR spectra were recorded in a Thermo Nicolet-5700 FTIR spectrophotometer (USA). The mild steel specimens of size 2.5 cm × 2.0 cm × 0.25 cm were prepared as described above. These specimens were immersed for 3 h in 100 mL of 1 M HCl solution containing 1.36×10^{-6} M SB. In order not to damage the protective film/or layer of the mild steel surfaces, the FTIR reflectance accessory was applied to study the mild steel surface.

Quantum chemical calculations for the molecular parameters related to SB were done using unrestricted Kohn–Sham formalism at density functional theory (DFT) level. For all DFT calculations, the Perdew–Burke–Ernzerhof (PBE1) functional [20] was used. We have chosen PBE1 functional because it has many times proved its efficiency on a wide range of compounds, and it generally provides accurate results on ground and excited-state properties, including charge-transfer transitions [21]. The split valence 6-31G** basis sets were used for all atoms and quantum chemical calculations were performed with the help of Gaussian 03 package [22]. We have performed all calculations in gas phase.

3 Results and discussion

3.1 Electrochemical impedance measurements

An electrochemical impedance result of mild steel/hydrochloric acid interface obtained in the absence and in the presence of various concentrations of SB in the form of Nyquist plots is shown in Fig. 1a. The Nyquist plots for all SB concentrations are characterized by one semicircular capacitive loop. The presence of inhibitor introduces the diffusion step in corrosion process and the reaction becomes diffusion-controlled. Hence, the corrosion process can have two steps as in any electrochemical process at the electrochemical interface, first, the oxidation of the metal (charge transfer process) and second, the diffusion of the metallic ions from the metal surface to the solution (mass transport process). Inhibitor gets adsorbed on the electrode surface and thereby produces a barrier for the metal to diffuse out to the bulk and this barrier increases with increasing the inhibitor concentration [23].

The diameter of the semicircular capacitive loop (Fig. 1a), the impedance of the double layer (Fig. 1b), phase angle (Fig. 1c) increased with increasing concentration of the SB. The general overview of the electrochemical impedance results meets the expectations from the theory of the technique, but it must be noted that the capacitive loops are depressed ones with centers under the real axis even though they have a semicircle appearance. Deviations of this kind are mostly referred to as frequency dispersion and they are attributed to irregularities and heterogeneities of the solid surfaces [5, 24]. In addition in the real corrosion systems, the double layer on the interface of metal/solution does not behave as a real capacitor. On the metal side of the double layer, the charge distribution is controlled by electron, whereas on the solution side it is controlled by ions [25]. The high frequency part of the impedance and phase angle reflects the behavior of heterogeneous surface layer, whereas the low frequency part shows the kinetic response for the charge transfer reaction.

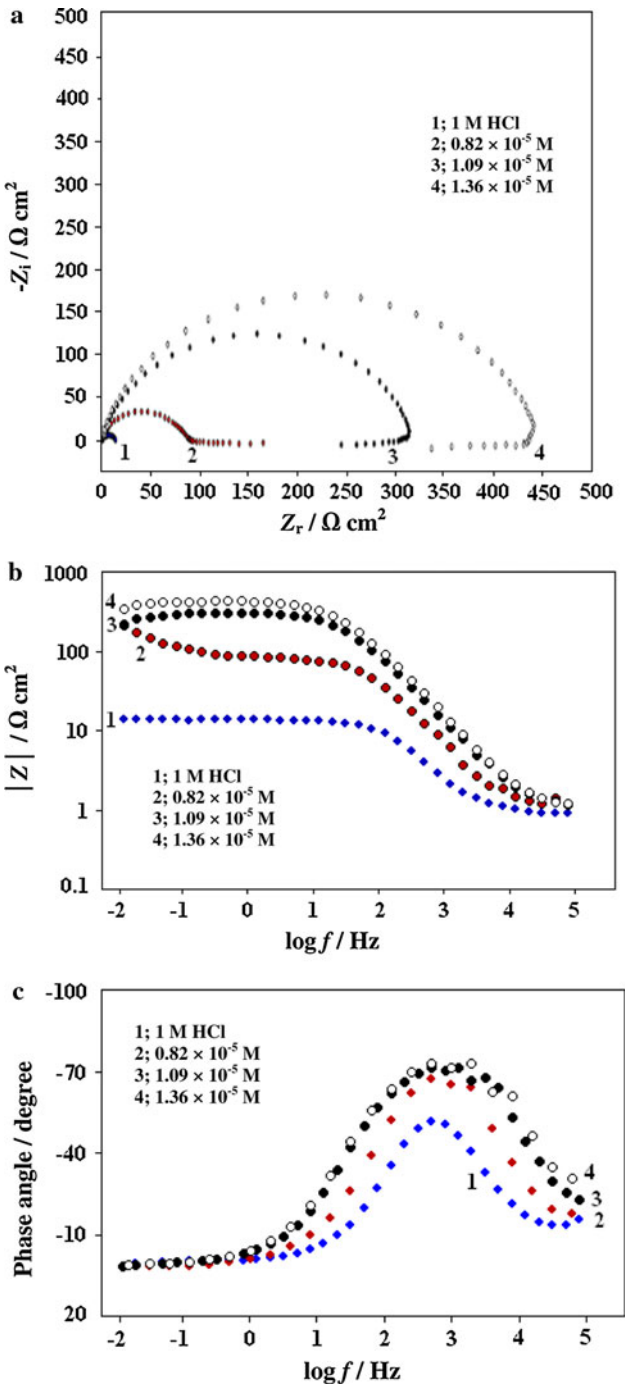

Fig. 1 Typical **a** Nyquist, **b** Bode-impedance and **c** phase angle plots obtained for the mild steel in 1 M HCl in the absence and presence of three different concentrations of SB

A diffusion tail can be seen for both uninhibited and inhibited solutions (Fig. 1a). The presence of this low frequency diffusion tail may be attributed to the relaxation process obtained by adsorption of species like $(Cl^-)_{ads}$ and $(H^+)_{ads}$ on the electrode surface [26, 27].

For the appraisal of the experimental results, equivalent circuit models, which physically correctly represent the systems under investigation, must be applied. The simplest model consists of the solution resistance, R_s, in series with the parallel combination of constant phase element (CPE) in place of double layer capacitance (C_{dl}) and charge transfer resistance (R_t). Such equivalent circuit (Fig. 2) has been used previously to model the mild steel/acid interface [28, 29]. The charge transfer resistance (R_p) must be corresponding to the resistance between the metal and OHP (outer Helmholtz plane) and can be calculated from the difference in impedance at lower and higher frequencies, as suggested by Tsuru et al. [30].

Mathematically, a CPE's impedance is given by

$$Z_{CPE} = Q^{-1}\,(j\omega)^{-n} \tag{1}$$

where Q is the magnitude of the CPE, j is the imaginary unit, ω is the angular frequency ($\omega = 2\pi f$, the frequency in Hz) and n is the phase shift which gives details about the degree of surface inhomogeneity. When $n = 1$, this is the same equation as that for the impedance of a capacitor, where $Q = C_{dl}$. In fact, when n is close to 1, the CPE resembles a capacitor, but the phase angle is not 90°. It is constant and somewhat less than 90° at all frequencies.

In spite of the mentioned fact, the term, double layer capacitance, is still often used in the evaluation of electrochemical impedance results to characterize the double layer believed to be formed at the metal/solution interface of systems displaying non-ideal capacitive behavior. For providing simple comparison between the capacitive behaviors of different corrosion systems, the values of Q were converted to C_{dl}. Hsu and Mansfeld [31] have given following equation for calculating the 'true' capacitance (C_{dl}):

$$C_{dl} = Q\,(\omega_{max})^{n-1} \tag{2}$$

here, ω_{max} represents the frequency at which the imaginary component reaches a maximum. It is the frequency at the top of the depressed semicircle, and it is also the frequency at which the real part (Z_r) is midway between the low and high frequency x-axis intercepts. The values of inhibition efficiency ($\mu_{IM}\%$) using R_t values were calculated as described previously [6].

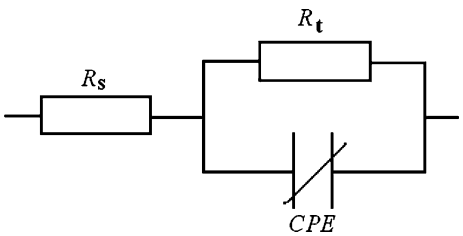

Fig. 2 The electrochemical equivalent circuit used to fit the impedance measurements that include a solution resistance (R_s), a constant phase element (CPE) and a polarization resistance or charge transfer (R_t)

Use of CPE in place of C_{dl} in the equivalent circuit model representing the metal/solution interface leads that the center of the capacitive loop rotates below the real axis up to a frequency independent constant phase angle (Fig. 1a) [32]. The value of which can be used as a measure of deviation from an ideal capacitive behavior.

The electrochemical impedance parameters extracted from the Nyquist plots for mild steel in 1 M HCl containing different concentrations of SB are given in Table 1. It is apparent that, the impedance response for mild steel in 1 M HCl changes significantly with increasing inhibitor concentration. It is worthy noting that the similar profile of the Nyquist plots is observed in the absence and presence of the inhibitor, indicating that the addition of inhibitors do not change the mechanism for the dissolution of mild steel in 1 M HCl. Table 1 shows that the addition of the SB into the corrosive solution caused to an increase in the inhibition efficiency, charge transfer resistance and a decrease in the double layer capacitance (C_{dl}) given as [33].

$$C_{dl} = \frac{\varepsilon\varepsilon_0 A}{d} \tag{3}$$

where ε_0 is the vacuum dielectric constant, ε is the local dielectric constant, d is the thickness of the double layer, and A is the surface area of the electrode. According to Eq. 2, a decrease in C_{dl} can happen if the inhibitor molecules (low dielectric constant) replace the adsorbed water molecules (high dielectric constant) on the mild steel surface. The capacitance is inversely proportional to the thickness of the double layer. Thus, decrease in the C_{dl} values could be attributed to the adsorption of SB on the metal surface. Decrease in the capacitance, which can result from a decrease in the local dielectric constant and/or an increase in the thickness of the electrical double layer, strongly suggests that the inhibitor molecules adsorbed at the metal/solution interface. In the absence and in the presence of inhibitor, phase shift value remains more or less identical; this indicates that the charge transfer process controls the dissolution mechanism [34] of mild steel in 1 M HCl solution in the absence and in the presence of SB.

In acidic solutions, it is known that inhibitor molecules can be protonated. Thus in solution both neutral molecule and cationic forms of inhibitor exist [35, 36]. In hydrochloric acid solutions, anodic dissolution of iron takes following steps:

(i)

$$Fe + Cl^- \rightleftarrows (FeCl^-)_{ads}$$

(ii)

$$(FeCl^-)_{ads} \rightleftarrows (FeCl)_{ads} + e^-$$

(iii)

$$(FeCl)_{ads} \rightarrow (FeCl^+) + e^-$$

(iv)

$$(FeCl^+) \rightleftarrows Fe^{++} + Cl^-$$

And cathodic hydrogen evolution takes following steps:

(v)

$$Fe + H^+ \rightleftarrows (FeH^+)_{ads}$$

(vi)

$$(FeH^+)_{ads} + e^- \rightarrow (FeH)_{ads}$$

(vii)

$$(FeH)_{ads} + H^+ + e^- \rightarrow Fe + H_2$$

It is assumed that Cl^- ion is first adsorbed onto the positively charged metal surface by coulombic attraction and then inhibitor molecules can be adsorbed through electrostatic interactions between the positively charged molecules and the negatively charged metal surface [35]. These adsorbed molecules interact with $(FeCl^-)_{ads}$ species to form monomolecular layers (by forming a complex) on the steel surface. These layers protect mild steel surface from attack by chloride ions. Thus the oxidation reaction of $(FeCl^-)_{ads}$ as shown by step (ii) → (vi) can be prevented. On the other hand, the protonated inhibitor molecules are also adsorbed at cathodic sites in competition with hydrogen ions that going to reduce hydrogen evolution.

Inhibition performance of the SB for mild steel/solution interface depends on several factors such as the number of adsorption sites, molecular size, and mode of interaction with the metal surface and extent of formation of metallic complexes [37]. The adsorption of SB at the mild steel surface can take place through its active centres; azomethine group (C=N), benzene rings and hetero-atoms (N, O, and S) and in addition to pi-electron interaction of the benzene rings with unshared d electrons of iron atoms.

Table 1 Electrochemical impedance parameters and the corresponding inhibition efficiencies for mild steel in 1 M HCl solution in the absence and presence of three different concentrations of Schiff base compound

Inhibitor ($M \times 10^{-6}$)	R_S (Ω cm^2)	R_t (Ω cm^2)	n	Q (μF cm^{-2})	C_{dl} (μF cm^{-2})	μ_{R_t} (%)
1 M HCl	0.88	12.2	0.842	282.2	97.7	–
0.82	1.11	95.4	0.855	84.4	35.5	87.2
1.09	1.07	295.8	0.865	39.5	19.9	95.9
1.36	0.96	419.4	0.867	31.6	16.6	97.1

3.2 Potentiodynamic polarization measurements

The typical Tafel polarization curves of mild steel in 1 M HCl in the presence and absence of SB at different

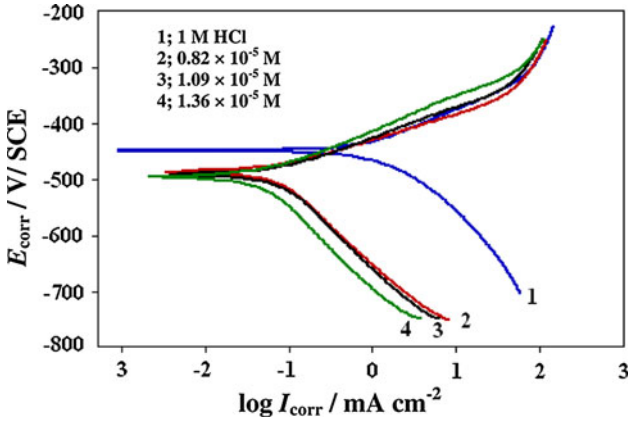

Fig. 3 Typical polarization curves for corrosion of mild steel in 1 M HCl in the absence and presence of three different concentrations of SB

concentrations are shown in Fig. 3. It could be observed that both the cathodic and anodic reactions were suppressed with the addition of SB, which suggests that the SB reduced anodic dissolution and also retarded the hydrogen evolution reaction effectively.

Various corrosion kinetics parameters, i.e. corrosion potential (E_{corr}), cathodic and anodic Tafel slopes (b_c, b_a) and corrosion current density (I_{corr}) obtained from the Tafel extrapolation of the polarization curves, are given in Table 2. The value of inhibition efficiency ($\mu_P\%$) was calculated from I_{corr} values as described previously [6]. The obtained results show that the inhibition efficiency increased, while the corrosion current density decreased when the concentration of the inhibitor is increased. This could be explained on the basis of adsorption of SB on the mild steel surface and the adsorption process enhanced with increasing inhibitor concentration. The data in Table 2 show that increasing SB concentration slightly shifts the values of corrosion potential (E_{corr}) in cathodic direction indicating that it acts as mixed-type inhibitor. From Table 2, it is clear that the values of both anodic and cathodic Tafel slope constants remain more or less identical with increasing SB concentration in the absence and in the presence of SB. This suggests that inhibitor does not participate in the mechanism of corrosion.

Table 2 Electrochemical polarization parameters and the corresponding inhibition efficiencies for mild steel in 1 M HCl solution in the absence and presence of three different concentrations of Schiff base compound

Inhibitor ($M \times 10^{-6}$)	E_{corr} (mV/ SCE)	I_{corr} ($\mu A\ cm^{-2}$)	b_a (mV dec^{-1})	b_c (mV dec^{-1})	μ_P (%)
1 M HCl	−448	1100	66.0	97.7	–
0.82	−486	76.8	45.7	119.2	93.0
1.09	−491	60.5	58.2	146.7	94.5
1.36	−495	52.8	63.1	121.2	95.2

3.3 Weight loss measurements

3.3.1 Effect of inhibitor concentration

Table 3 shows the corrosion parameters, adsorption equilibrium constant (K_{ads}) and free energy of adsorption (ΔG°_{ads}) obtained from weight loss studies for the mild steel in 1 M HCl solution in the absence and presence of different concentrations of SB. The inhibition efficiency ($\mu_{WL}\%$) and corrosion rate (C_R, mm $year^{-1}$) were calculated as described previously [6]. K_{ads} and ΔG°_{ads} were calculated as given in latter section.

It can be observed that $\mu_{WL}\%$ increases and corrosion rate decreases as inhibitor concentration increased from 0.14×10^{-6} to 1.36×10^{-6} M. This behavior is the result of increased adsorption and increased coverage of inhibitor on the mild steel surface with increase in the inhibitor concentration. The results obtained from the weight loss measurements are in reasonably good agreement with those obtained from the electrochemical impedance and the polarization measurements.

3.3.2 Effect of temperature

The effect of temperature on the inhibition performance of SB for mild steel in 1 M HCl solution in the absence and presence of 1.36×10^{-6} M concentration at temperature ranging from 308 to 338 K was studied using weight loss measurements. The results are presented in Table 4. The inhibition efficiencies ($\mu_{WL}\%$) are almost constant and on the other hand there is a small increase (from 0.37 to 8.16 mm $year^{-1}$) in corrosion rate with increasing solution temperature from 308 to 338 K. The adsorption and desorption processes occur in opposite direction simultaneously at equilibrium. Various factors such as solution temperature, inhibitor concentration determines the direction in which this equilibrium will shift. At higher temperature more desorption of inhibitor molecules takes place from metal/solution interface. This increase in desorption is the cause of increased corrosion rate with temperature. Table 4 shows that corrosion rate increases more rapidly with temperature in the absence of the inhibitor. These results confirm that SB is an excellent corrosion inhibitor for mild steel in 1 M HCl in the range of temperature studied.

3.3.3 Effect of exposure time

In order to study the stability of adsorbed inhibitor film at mild steel/acid solution interface with time, weight loss measurements were conducted at 308 K for 3–24 h

Table 3 Corrosion parameters and free energy of adsorption obtained from weight loss measurements for mild steel in 1 M HCl in presence of different concentrations of Schiff base compound at 308 K

Inhibitor ($\times 10^{-6}$ M)	Weight loss (mg cm^{-2} h^{-1})	C_R (mm year^{-1})	μ_{WL} (%)	K_{ads} ($\times 10^5$ M^{-1})	ΔG°_{ads} (kJ mol^{-1})
1 M HCl	7.00	77.9	–	–	–
0.14	1.63	18.2	76.7	2.4	−42.0
0.27	0.77	8.5	89.1	3.0	−42.6
0.54	0.13	1.5	98.1	9.5	−45.5
0.82	0.10	1.1	98.6	8.6	−45.3
1.09	0.07	0.7	99.0	9.1	−45.4
1.36	0.03	0.4	99.5	14.6	−46.6

Table 4 Various parameters obtained from weight loss measurements for mild steel in 1 M HCl in presence of 1.36 × 10^{-6} M Schiff base compound at various temperatures

Temp (K)	1 M HCl			Schiff base compound						
	C_R (mm year^{-1})	λ (mg cm^{-2} h^{-1})	E_a (kJ mol^{-1})	C_R (mm year^{-1})	μ_{WL} %	ΔG°_{ads} (kJ mol^{-1})	λ (mg cm^{-2} h^{-1})	E_a (kJ mol^{-1})	ΔH°_{ads} (kJ mol^{-1})	ΔS°_{ads} (kJ mol^{-1})
308	77.9			0.4	99.5	−46.7				−50.7
318	107.6	6.83 × 10^6	29.2	0.7	99.3	−47.3	5.69 × 10^{14}	92.1	−62.3	−47.1
328	162.5			3.0	98.2	−46.2				−49.1
338	208.5			8.2	96.1	−45.3				−50.1

exposure time in 1 M HCl containing 1.36 × 10^{-6} M SB. The effect of exposure time on inhibition efficiency is shown in Fig. 4. Inspection this figure reveals that a small decrease was found in inhibition efficiency from 99.5 to 86.5% as exposure time increases from 3 to 24 h. A slight decrease in inhibition after 24 h is probably due to decreased adsorption and increased desorption. Shriver et al. [38] explained that decrease in inhibition for long period of immersion can be attributed to the depletion of available inhibitor molecules in the solution due to chelate formation between iron and the inhibitor ligands. Thus we can conclude that studied compound is efficient corrosion inhibitors for mild steel in molar hydrochloric acid solution.

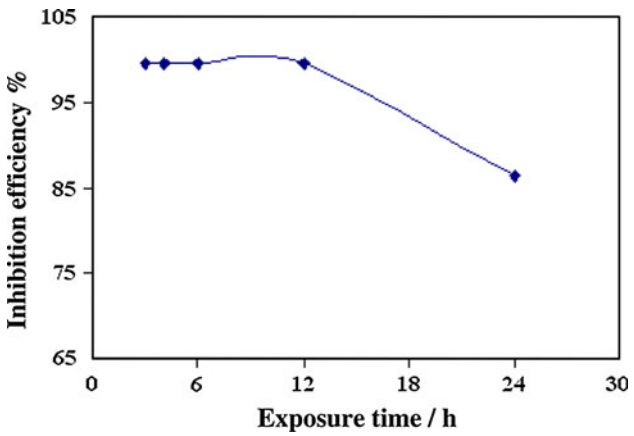

Fig. 4 Plot of μ_{WL}% against exposure time for mild steel in 1 M HCl containing 1.36 × 10^{-6} M

3.3.4 *Activation energy and pre-exponential factor*

It is important to study thermodynamic parameters to get insight into the inhibitive mechanism. A plot of the logarithm of the corrosion rate (mm year^{-1}) of mild steel obtained from weight loss measurements vs. 1000/T gave a straight line as shown in Fig. 5a. The apparent activation energy (E_a) was calculated by using following Arrhenius equation:

$$C_R = \lambda \exp\left(-\frac{E_a}{RT}\right) \quad (4)$$

where E_a is the apparent activation energy for the corrosion of mild steel in 1 M HCl solution, R the general gas constant, λ the Arrhenius pre-exponential factor and T is the absolute temperature.

The values of E_a and λ obtained from the slope and intercept, respectively of the line (Fig. 5a) are given in Table 4. The linear regression coefficients (R^2) are close to 1, indicating that the corrosion of mild steel in 1 M HCl solution may be elucidated using the kinetic model. Table 4 shows that the values of E_a and λ for inhibited solution are higher than that for uninhibited solution. The higher values of E_a suggest that dissolution of mild steel is slow in presence of inhibitors. It is clear from Eq. 4 that the

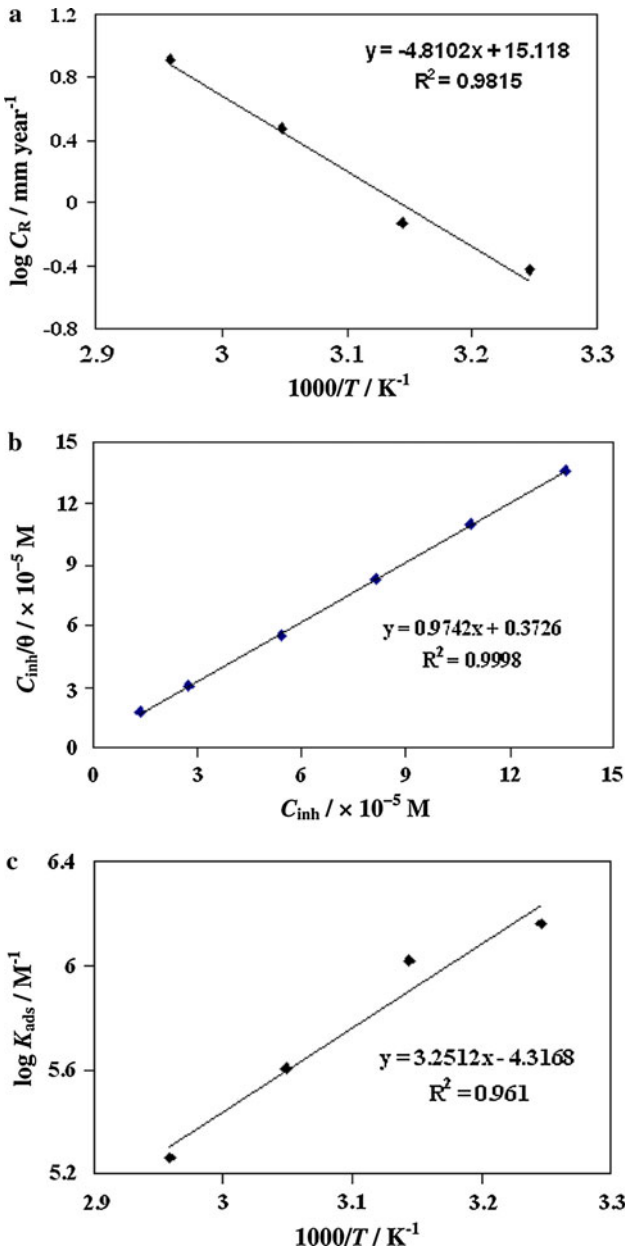

Fig. 5 **a** Arrhenius plots of log C_R vs. 1000/T; **b** Langmuir adsorption isotherm plot; and **c** plot of log K_{ads} vs. 1000/T for the adsorption of the SB at mild steel/hydrochloric acid interface

higher E_a and the lower λ lead to the lower corrosion rate. In general, the effect of E_a on mild steel corrosion is larger than that of λ. In the present study, values of E_a and λ vary in similar manner and therefore, the combined effect of E_a and λ results in the increase of corrosion rate with temperature.

3.3.5 *Adsorption isotherm and thermodynamic parameters*

It is well established that the first step in corrosion inhibition of metals and alloys is the adsorption of organic inhibitor molecules at the metal/solution interface and that the adsorption depends on the molecule's chemical composition, the temperature and the electrochemical potential at the metal/solution interface. In fact, the solvent water molecules could also adsorb at metal/solution interface. So the adsorption of organic inhibitor molecules from the aqueous solution can be regarded as a quasi-substitution process between the organic compounds in the aqueous phase [$Org_{(sol)}$] and water molecules at the electrode surface [$H_2O_{(ads)}$] [39]

$$Org_{(sol)} + xH_2O_{(ads)} \leftrightarrow Org_{(ads)} + xH_2O_{(sol)} \quad (5)$$

where x is the size ratio, that is, the number of water molecules replaced by one organic inhibitor.

Basic information on the interaction between the inhibitor and the alloy surface can be provided by the adsorption isotherm. In order to obtain the isotherm, the fractional coverage values θ as a function of inhibitor concentration (C_{inh}) must be obtained. It is well known that θ can be obtained from the μ_{WL}%/100 ratio. Attempts were made to fit the θ values to various isotherms including Langmuir, Temkin, Frumkin and Flory–Huggins. Many adsorption isotherms were plotted and the Langmuir adsorption isotherm was found to be the best description of the adsorption behavior of the studied inhibitors. According to this isotherm, θ is related to equilibrium adsorption constant (K_{ads}) and C_{inh} by the relation

$$\frac{C_{inh}}{\theta} = \frac{1}{K_{ads}} + C_{inh} \quad (6)$$

Figure 5b shows the plot of C_{inh}/θ vs. C_{inh} and the expected linear relationship is obtained. The value of regression coefficient (R^2) confirmed the validity of this approach. The slope of this straight line is 0.974, suggesting that adsorbed inhibitor molecules form monolayer on the mild steel surface and there is no interaction among the adsorbed inhibitor molecules. On the other hand, the equilibrium constant of adsorption is related to the standard energy of adsorption (ΔG°_{ads}) by the relation [40]

$$K_{ads} = \left(\frac{1}{55.5}\right) \exp\left(-\frac{\Delta G^\circ_{ads}}{RT}\right) \quad (7)$$

where R is the universal gas constant, T the absolute temperature and the value of 55.5 is the concentration of water in mol l^{-1} in the solution [41].

The values of K_{ads} obtained from Eq. 7 are listed in Table 3, together with the values of ΔG°_{ads}. The values of K_{ads} and ΔG°_{ads} increase with increasing inhibitor concentration, suggesting stronger interaction between inhibitor molecules and iron surface atoms. The high value of these parameters for studied compound indicates stronger and more stable adsorbed layer is formed at mild steel/acid solution interface, which results in the higher inhibition

efficiency [42]. Furthermore, the values of ΔG°_{ads} for the Schiff base compound are negative (Table 3) and these values are consistent with the spontaneity of the adsorption process and the stability of the adsorbed layer on the mild steel surface [43]. Generally, ΔG°_{ads} values of -20 kJ mol^{-1} or higher are associated with an electrostatic interaction between charged molecules and charged metal surface, physisorption; those of -40 kJ mol^{-1} or lower involve charge sharing or transfer from the inhibitor molecules to the metal surface to form a coordinate covalent bond, chemisorption [44]. The values of ΔG°_{ads} for investigated compound SB were found to be almost constant (-47.3 to -45.3 kJ mol^{-1}) at a temperature range 308–338 K (Table 4). This indicated that the adsorption of investigated compound SB at mild steel/hydrochloric acid interface is a typical chemisorption. This chemisorption mechanism can be attributed to the donation of pi-electron by the azomethine group, aromatic rings, and nonbinding electron pairs of hetero-atoms as reactive centers. The adsorption of inhibitor molecules on the mild steel surface can be explained on the ground of donor acceptor interaction between electron density of azomethine group, aromatic rings, hetero-atoms of inhibitor and vacant d-orbitals of iron atoms at the mild steel surface [6, 45].

The heat of adsorption and entropy of adsorption are important parameters in studying adsorption of organic inhibitors at metal/solution interface. The heat of adsorption (ΔH) is calculated using the Van't Hoff equation:

$$\ln K = \frac{-\Delta H}{RT} + \text{constant} \tag{8}$$

Figure 5c shows the straight lines of plot of log K_{ads} vs. $1/T$ and slope of this straight line is equal to $-\Delta H_{ads}/2.303R$. The heat of adsorption could be approximately regarded as the standard heat of adsorption (ΔH°_{ads}) under experimental conditions [46]. Now standard entropy of adsorption (ΔS°_{ads}) is obtained by the thermodynamic basic equation:

$$\Delta S^{\circ}_{ads} = \frac{\Delta H^{\circ}_{ads} - \Delta G^{\circ}_{ads}}{T} \tag{9}$$

All the calculated thermodynamic parameters are listed in Table 4. It has been found that values of ΔH°_{ads} are negative, suggesting that the adsorption of inhibitor is an exothermic process [47]. The values of ΔS°_{ads} are nearly constant and negative, ranging between -50.7 and -47.1 J K^{-1} mol^{-1} at a temperature range 308–338 K. This is expected one, since adsorption is an exothermic process and is always accompanied by a decrease of entropy. The decrease in entropy suggested that in the rate determining step there is an association rather than dissociation.

Table 5 Prominent peaks obtained from FTIR spectroscopy

Frequency (cm^{-1})	Band assignment
FTIR of pure SB	
1136	C–O str
1290	C=S str
1384, 1544	C=C str (aromatic rings)
1625	C=N str
1727	C=O str
2603	O–H str (COOH)
2983	Ar–H str
3447	N–H str
FTIR of SB on mild steel	
1113	C–O str
1263	C=S str
1356, 1479	C=C str (aromatic rings)
1552	C=N str
1683	C=O str
2858	O–H str (COOH)
2971	Ar–H str
3320	N–H str

3.4 FTIR study

It is well established that FTIR spectrophotometer is a powerful instrument that can be used to determine the functional group present in organic compounds as well as the type of bonding for organic inhibitors absorbed on the metal surface. The prominent peaks obtained from FTIR analysis of pure SB and SB on mild steel are given in Table 5. In present study, FTIR spectra were used to support the fact that corrosion inhibition of mild steel in acid media is due to the adsorption of inhibitor molecules at the mild steel/hydrochloric acid interface and adsorption occurred by interaction of surface iron atoms and active centres of inhibitor molecules.

3.5 Quantum chemical calculations

In order to correlate experimental data obtained from different techniques (viz., electrochemical and weight loss) for SB and its structural and electronic properties, quantum chemical properties such as energy of highest occupied molecular orbital (E_{HOMO}), energy of lowest unoccupied molecular orbital (E_{LUMO}), HOMO–LUMO energy gap (ΔE_{L-H}), vertical ionisation potential (IP), vertical electron affinity (EA), molecular band gap (ΔE_{MBG}) and number of transferred electrons (ΔN) has been computed. These computed parameters are listed in Table 6. The vertical ionization potential (IP) and vertical electron affinity (EA) were computed using unrestricted Kohn–Sham formalism. The molecular band gap was computed as the first vertical

Table 6 The computed molecular parameters for Schiff base compound

	E_{HOMO} (eV)	E_{LUMO} (eV)	ΔE_{L-H} (eV)	ΔE_{MBG} (eV)	IP (eV)	EA (eV)	μ_{WL} %	ΔN
Fexofenadine	−5.63	−1.98	3.65	1.9	6.94	−0.78	99.5	0.88
Iron[a]	−7.81	−0.25	7.69[b]	–	–	–	–	–
			2.32[c]					

[a] HOMO and LUMO values for iron were taken as ionization potential and electron affinity, respectively [5]

[b] $LUMO_{(base)}$–$HOMO_{(acid)}$

[c] $LUMO_{(acid)}$–$HOMO_{(base)}$

electronic excitation energy from the ground state using the time-dependent density functional theory (TD-DFT) approach as implemented in Gaussian 03. The findings of our previous studies [12] have shown that the molecular band gap is fundamentally more appropriate (than HOMO–LUMO energy gap) to correlate inhibition properties of compounds.

It has been reported that E_{HOMO} is often associated with the electron donating ability of a molecule, whereas E_{LUMO} indicates its ability to accept electrons. The high values of E_{HOMO} are likely to indicate a tendency of the molecule to donate electrons to appropriate acceptor molecules with low energy and empty molecular orbital. Figure 6 shows the full optimized minimum energy structure of SB.

The bonding tendencies of the inhibitors towards the metal surface atoms can be discussed in terms of the HSAB (hard–soft–acid–base) [48, 49] and the frontier-controlled interaction concepts [49, 50]. According to the general rule of HSAB principle, hard acids prefer to coordinate to hard bases and soft acids prefer to co-ordinate to soft bases. Furthermore, metallic atoms are known to be soft acids, and hard molecules have a large HOMO–LUMO energy gap and soft molecules have a small HOMO–LUMO energy gap. In the present study the HOMO–LUMO energy gap is 3.648 eV mol^{-1} (Table 6), suggesting that SB is a soft molecule and this results in high corrosion inhibition implying soft–soft interaction. According to molecular orbital (MO) theory, similar result can also be found. Since iron atom (acid) is the electron pair acceptor and inhibitor (base) is the electron pair donor, the energy difference of the LUMO (HOMO is nothing special) of the acid and the HOMO (LUMO is nothing special) of the base must be considered. MO theory suggests that the overlap between the $LUMO_{(acid)}$ and the $HOMO_{(base)}$ is governing factor in bonding [51]; the lower the HOMO–LUMO energy gap the higher HOMO–LUMO overlap and the stronger base–acid bond formation and consequently the higher inhibition efficiency. With these results in mind, the energy data in Table 6 together with molecular band gap also suggest that SB is an efficient inhibitor for mild steel corrosion in molar hydrochloric acid solution.

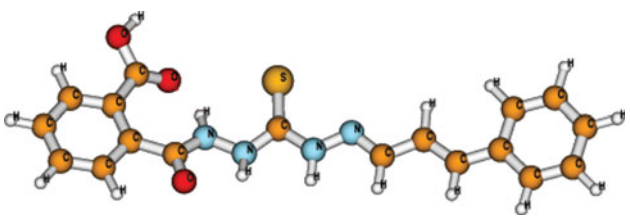

Fig. 6 Optimized structure of SB

In addition the number of transferred electrons (ΔN) was also calculated depending on the quantum chemical method [52]:

$$\Delta N = \frac{(\chi_{Fe} - \chi_{inh})}{2(\eta_{Fe} + \eta_{inh})} \tag{10}$$

where χ_{Fe} and χ_{inh} denote the absolute electronegativity of iron and the inhibitor molecule, respectively; η_{Fe} and η_{inh} denote the absolute hardness of iron and the inhibitor molecule, respectively. These quantities are related to electron affinity (A) and ionization potential (I) as follows:

$$\chi = (I + A)/2; \quad \eta = (I - A)/2 \tag{11}$$

IP and EA are related [48] in turn to E_{HOMO} and E_{LUMO} as follows:

$$I = -E_{HOMO}; \quad A = -E_{LUMO} \tag{12}$$

For iron atom, a theoretical χ value of 7 eV mol^{-1} and η value of 0 eV mol^{-1} were used [51] to calculate the number of electrons transferred (ΔN) from inhibitor to the iron atom. The number of transferred electrons depends strongly on what the actual quantum chemical method employed for computation. Furthermore, the expression "number of transferred electrons" is the wording "electron-donating ability", which does not imply that the figures of ΔN actually indicate the number of electrons leaving the donor and entering the acceptor molecule.

Using Eq. 10, the value of electron-donating ability (ΔN) was calculated and its value is given in Table 6. If $\Delta N < 3.6$ (electron), the inhibition efficiency increases with increasing value of ΔN, while it decreased if $\Delta N > 3.6$ (electron) [52, 53]. In present contribution, SB is the donor of electrons, and the iron surface atom was the

acceptor. The SB was bound to the mild steel surface, and thus formed inhibition adsorption layer against corrosion at mild steel/hydrochloric acid solution interface.

3.6 Mechanism of adsorption and inhibition

The transition of metal/solution interface from a state of active dissolution to the passive state can be attributed to the adsorption of the inhibitor molecules at the metal/solution interface, forming a protective film. The rate of adsorption is usually rapid and hence, the reactive metal surface is shielded from the aggressive environment [54]. It is well recognised that organic inhibitor molecules set up their inhibition action via the adsorption of the inhibitor molecules onto the metal/solution interface. Adsorption process can occur through the replacement of solvent molecules from metal surface by ions and molecules accumulated in the vicinity of metal/solution interface. Ions can accumulate at the metal/solution interface in excess of those required to balance the charge on the metal at the operating potential. These ions replace solvent molecules from the metal surface and their centres reside at the inner Helmholtz plane. This phenomenon is termed specific adsorption, contact adsorption. The anions are adsorbed when the metal surface has an excess positive charge in an amount greater than that required to balance the charge corresponding to the applied potential. Aromatic compounds (which contain the benzene ring) undergo particularly strong adsorption on many electrode surfaces. The bonding can occur between metal surface atoms and the aromatic ring of the adsorbate molecules or ligands substituent groups. The exact nature of the interactions between a metal surface and an aromatic molecule depends on the relative coordinating strength towards the given metal of the particular groups present [55].

The adsorption of Schiff base compound (SB) at mild steel/hydrochloric acid interface can be attributed to the presence of hetero atoms (N, O and S), azomethine group and aromatic rings. Thus, the possible reaction centres are unshared electron pair of hetero-atoms and π-electrons of azomethine group and aromatic rings. The adsorption of SB at mild steel/1 M HCl interface can be explained as follows. Schiff base molecules might be protonated in the acid solution as

$$[C_{18}H_{16}N_4O_3S] + xH^+ \rightarrow [C_{18}H_{16}N_4O_3SH_x]^{x+} \quad (13)$$

In aqueous acidic solutions, the SB molecules exist either as neutral molecules or in the form of protonated molecules (cations). SB may adsorb on the metal/acid solution interface by one and/or more of the following ways: (i) electrostatic interaction of protonated Schiff base compound with already adsorbed chloride ions (synergistic effect), (ii) donor–acceptor interactions between the π-electrons of aromatic ring and vacant d orbital of surface iron atoms, (iii) interaction between unshared electron pairs of hetero atoms and vacant d-orbital of iron surface atoms.

Two modes of adsorption are generally considered on the surface of metal. In one mode, the neutral Schiff base compound may be adsorbed on the surface of mild steel through the chemisorption mechanism, involving the displacement of water molecules from the mild steel surface and the sharing electrons between the hetero atoms and iron. The inhibitor molecules can also adsorb on the mild steel surface on the basis of donor–acceptor interactions between π-electrons of the aromatic ring and vacant d-orbitals of surface iron atoms. In second mode, since it is well known that the steel surface bears positive charge in acid solution [56], so it is difficult for the protonated Schiff base compound to approach the positively charged mild steel surface (H_3O^+/metal interface) due to the electrostatic repulsion. Since chloride ions have a smaller degree of hydration, thus they could bring excess negative charges in the vicinity of the interface and favour more adsorption of the positively charged inhibitor molecules, the protonated Schiff base compound adsorb through electrostatic interactions between the positively charged molecules and the negatively charged metal surface. Thus there is a synergism between adsorbed Cl^- ions and protonated Schiff base compound. The excellent performance of investigated Schiff base compound (SB) is attributed to the presence of hetero-atoms, azomethine group, aromatic rings and planarity of the compound (Fig. 6) [57].

4 Conclusions

1. SB acted as an efficient inhibitor for the corrosion of mild steel in 1 M HCl and exhibited 99.5% efficiency at concentration of 1.36×10^{-6} M.
2. The electrochemical impedance study showed that corrosion inhibition of mild steel in molar hydrochloric acid solution takes place by adsorption process. Tafel polarization curves indicated that the SB is a mixed-type inhibitor.
3. The large negative values of ΔG°_{ads} indicated that adsorption of studied drug on the mild steel surface is spontaneous and adsorption mechanism is a typical chemisorption.
4. The adsorption of the SB on the mild steel/solution interface obeyed Langmuir adsorption isotherm. The high values of K_{ads} suggested that studied compound is strongly adsorbed and adsorbed inhibitor film at the mild steel/hydrochloric acid interface is stable.
5. The calculated quantum chemical parameters such as E_{L-H}, E_{HOMO}, E_{LUMO}, ΔE_{MBG}, IP, EA and ΔN support the good inhibiting performance of SB.

6. The FTIR spectrum showed that the inhibition is due to the formation of the film at the metal/acid solution interface through adsorption of SB molecules.

Acknowledgment One of the authors, Ishtiaque Ahamad gratefully acknowledges the financial support of University Grant Commission (U.G.C.), New Delhi provided as Senior Research Fellowship.

References

1. Schmitt G (1984) Application of inhibitors for acid media. Br Corros J 19:165–176
2. Zucchi F, Trabanelli G, Brunoro G (1994) Iron corrosion inhibition in hot 4 M HCl solution by t-cinnamaldehyde and its structure-related compounds. Corros Sci 36:1683–1690
3. Quraishi MA, Jamal D (2000) Dianils: new and effective corrosion inhibitors for oil-well steel (N-80) and mild steel in boiling hydrochloric acid. Corrosion 56:156–160
4. Hasanov R, Sadıkoglu M, Bilgic S (2007) Electrochemical and quantum chemical studies of some Schiff bases on the corrosion of steel in H2SO4 solution. Appl Surf Sci 253:3913–3921
5. Ozcan M (2008) AC impedance measurement of cystine adsorption at mild steel/sulfuric acid interface as corrosion inhibitor. J Solid State Electrochem 12:1653–1661
6. Ahamad I, Quraishi MA (2009) Bis (benzimidazol-2-yl) disulphide: an efficient water soluble inhibitor for corrosion of mild steel in acid media. Corros Sci 51:2006–2013
7. Ashassi-Sorkhabi H, Eshaghi M (2009) Corrosion inhibition of mild steel in hydrochloric acid by betanin as a green inhibitor. J Solid State Electrochem 13:1297–1301
8. Prabhu RA, Shanbhag AV, Venkatesha TV (2007) Influence of tramadol [2-[(dimethylamino)methyl]-1-(3-methoxyphenyl) cyclohexanol hydrate] on corrosion inhibition of mild steel in acidic media. J Appl Electrochem 37:491–497
9. Emregül KC, Hayvalı M (2004) Studies on the effect of vanillin and protocatechualdehyde on the corrosion of steel in hydrochloric acid. Mater Chem Phys 83:209–216
10. Bain CD, Troughton EB, Tao Y-T, Evall J, Whitesides GM, Nuzzo RG (1989) Formation of monolayer films by the spontaneous assembly of organic thiols from solution onto gold. J Am Chem Soc 111:321–335
11. Bilgic S, Caliskan N (2001) An investigation of some Schiff bases as corrosion inhibitors for austenitic chromium–nickel steel in H_2SO_4. J Appl Electrochem 31:79–83
12. Ahamad I, Prasad R, Quraishi MA (2010) Thermodynamic, electrochemical and quantum chemical investigation of some Schiff bases as corrosion inhibitors for mild steel in hydrochloric acid solutions. Corros Sci 52:933–942
13. Ashassi-Sorkhabi H, Seifzadeh D, Hosseini MG (2008) EN, EIS and polarization studies to evaluate the inhibition effect of 3H-phenothiazin-3-one, 7-dimethylamin on mild steel corrosion in 1 M HCl solution. Corros Sci 50:3363–3370
14. Govindaraju KM, Gopi D, Kavitha L (2009) Inhibiting effects of 4-amino-antipyrine based Schiff base derivatives on the corrosion of mild steel in hydrochloric acid. J Appl Electrochem 39:2345–2352
15. Shokry H, Yuasa M, Sekine I, Issa RM, El-Baradie HY, Gomma GK (1998) Corrosion inhibition of mild steel by Schiff base compounds in various aqueous solutions: part I. Corros Sci 40: 2173–2186
16. Kandemirli F, Sagdinc S (2007) Theoretical study of corrosion inhibition of amides and thiosemicarbazones. Corros Sci 49: 2118–2130
17. Parac M, Grimme S (2002) Comparison of multireference Møller-Plesset theory and time-dependent methods for the calculation of vertical excitation energies of molecules. J Phys Chem A 106: 6844–6850
18. Shen X, Wu D, Huang X, Liu Q, Huang Z, Kang B (1997) Copper complexes derived from 1-(2-carboxybenzoyl)thiosemicarbazide (H3L): syntheses, characterization and crystal structure of [Cu3L2(Py)6](HIm)$(H_2O)_2$. Polyhedron 16(1997):1477–1482
19. ASTM (1990) Standard practice for laboratory immersion corrosion testing of metals, 3.02, G 31-72. Annual Book of Standards
20. Perdew JP, Burke K, Ernzerhof M (1997) Generalized gradient approximation made simple. Phys Rev Lett 78:1396–1396 [Phys Rev Lett (1996) 77:3865]
21. Petit L, Maldivi P, Adamo C (2005) Predictions of optical excitations in transition-metal complexes with time dependent-density functional theory: influence of basis sets. J Chem Theory Comput 1:953–962 and reference cited therein
22. Frisch MJ, Trucks GW, Schlegel HB, Scuseria GE, Robb MA, Cheeseman JR, Montgomery JA, Vreven T Jr, Kudin KN, Burant JC, Millam JM, Iyengar SS, Tomasi J, Barone V, Mennucci B, Cossi M, Scalmani G, Rega N, Petersson GA, Nakatsuji H, Hada M, Ehara M, Toyota K, Fukuda R, Hasegawa J, Ishida M, Nakajima T, Honda Y, Kitao O, Nakai H, Klene M, Li X, Knox JE, Hratchian HP, Cross JB, Bakken V, Adamo C, Jaramillo J, Gomperts R, Stratmann RE, Yazyev O, Austin AJ, Cammi R, Pomelli C, Ochterski JW, Ayala PY, Morokuma K, Voth GA, Salvador P, Dannenberg JJ, Zakrzewski VG, Dapprich S, Daniels AD, Strain MC, Farkas O, Malick DK, Rabuck AD, Raghavachari K, Foresman JB, Ortiz JV, Cui Q, Baboul AG, Clifford S, Cioslowski J, Stefanov BB, Liu G, Liashenko A, Piskorz P, Komaromi I, Martin RL, Fox DJ, Keith T, Al-Laham MA, Peng CY, Nanayakkara A, Challacombe M, Gill PMW, Johnson B, Chen W, Wong MW, Gonzalez C, Pople JA (2004) Gaussian 03. Gaussian Inc., Wallingford
23. Satpati AK, Ravindran PV (2008) Electrochemical study of the inhibition of corrosion of stainless steel by 1,2,3-benzotriazole in acidic media. Mater Chem Phys 109:352–359
24. Juttner K (1990) Electrochemical impedance spectroscopy (EIS) of corrosion processes on inhomogeneous surfaces. Electrochim Acta 35:1501–1508
25. Ozcan M, Dehri I, Erbil M (2004) Organic sulphur-containing compounds as corrosion inhibitors for mild steel in acidic media: correlation between inhibition efficiency and chemical structure. Appl Surf Sci 236:155–164
26. Aoki IV, Guedes IG, Maranho SL (2002) Copper phthalocyanine as corrosion inhibitor for ASTM A606-4 steel in 16% hydrochloric acid. J Appl Electrochem 32:915–919
27. Hassan HH, Abdelghani E, Amin MA (2007) Inhibition of mild steel corrosion in hydrochloric acid solution by triazole derivatives: part I. Polarization and EIS studies. Electrochim Acta 52:6359–6366
28. Growcock FB, Jasinski JH (1989) Time-resolved impedance spectroscopy of mild steel in concentrated hydrochloric acid. J Electrochem Soc 136:2310–2314
29. Machnikova E, Whitmire KH, Hackerman N (2008) Corrosion inhibition of carbon steel in hydrochloric acid by furan derivatives. Electrochim Acta 53:6024–6032
30. Tsuru T, Haruyama S, Gijutsu B (1978) Corrosion monitor based on impedance method: construction and its application to homogeneous corrosion. J Jpn Soc Corros Eng 27:573–579
31. Hsu CS, Mansfeld F (2001) Concerning the conversion of the constant phase element parameter Y0 into a capacitance. Corrosion 57:747–748
32. Martinez S, Metikos-Hukovic M (2003) A nonlinear kinetic model introduced for the corrosion inhibitive properties of some organic inhibitors. J Appl Electrochem 33:11371142

33. Oguzie EE, Li Y, Wang FH (2007) Effect of 2-amino-3-mercaptopropanoic acid (cysteine) on the corrosion behaviour of low carbon steel in sulphuric acid. Electrochim Acta 53:909–914
34. Hermas AA, Morad MS, Wahdan MH (2004) Effect of PgTPhPBr on the electrochemical and corrosion behaviour of 304 stainless steel in H2SO4 solution. J Appl Electrochem 34:95–102
35. Quraishi MA, Rafiquee MZA, Khan S, Saxena N (2007) Corrosion inhibition of aluminium in acid solutions by some imidazoline derivatives. J Appl Electrochem 37:1153–1162
36. Popova A (2007) Temperature effect on mild steel corrosion in acid media in presence of azoles. Corros Sci 49:2144–2158
37. Emregul KC, Kurtaran R, Atakol O (2003) An investigation of chloride-substituted Schiff bases as corrosion inhibitors for steel. Corros Sci 45:2803–2817
38. Shriver DF, Atkins PW, Langford CH (1994) In: Inorganic chemistry, 2nd edn. Oxford University Press, Oxford, p 238
39. Sahin M, Bilgic S, Yilmaz H (2002) The inhibition effects of some cyclic nitrogen compounds on the corrosion of the steel in NaCl mediums. Appl Surf Sci 195:1–7
40. Kaminski M, Szklarska-Smialowska Z (1973) Adsorption of thiophene derivatives on steel in sulphuric acid solutions. Corros Sci 13:557–565
41. Olivares O, Likhanova NV, Gomez B, Navarrete J, Llanos-Serrano ME, Arce E, Hallen JM (2006) Electrochemical and XPS studies of decylamides of α-amino acids adsorption on carbon steel in acidic environment. Appl Surf Sci 252:2894–2909
42. Lagrenee M, Mernari B, Bouanis M, Traisnel M, Bentiss F (2002) Study of the mechanism and inhibiting efficiency of 3,5-bis(4-methylthiophenyl)-4H-1,2,4-triazole on mild steel corrosion in acidic media. Corros Sci 44:573–588
43. Fouda AS, Heakal FE, Radwan MS (2009) Role of some thiadiazole derivatives as inhibitors for the corrosion of C-steel in 1 M H_2SO_4. J Appl Electrochem 39:391–402
44. Hosseini M, Mertens SFL, Arshadi MR (2003) Synergism and antagonism in mild steel corrosion inhibition by sodium dodecylbenzenesulphonate and hexamethylenetetramine. Corros Sci 45:1473–1489
45. Donahue F, Nobe K (1965) Theory of organic corrosion inhibitors. J Electrochem Soc 112:886–891
46. Zhao TP, Mu GN (1999) The adsorption and corrosion inhibition of anion surfactants on aluminium surface in hydrochloric acid. Corros Sci 41:1937–1944
47. Li XH, Mu GN (2005) Tween-40 as corrosion inhibitor for cold rolled steel in sulphuric acid: weight loss study, electrochemical characterization, and AFM. Appl Surf Sci 252:1254–1265
48. Pearson RG (1988) Absolute electronegativity and hardness: application to inorganic chemistry. Inorg Chem 27:734–740
49. Koch E (2005) Acid–base interactions in energetic materials. I: The hard and soft acids and bases (HSAB) principle-insights to reactivity and sensitivity of energetic materials. Propellants Explos Pyrotech 30:5–16
50. Klopman G (1968) Chemical reactivity and the concept of charge and frontier-controlled reactions. J Am Chem Soc 90:223–234
51. Bentiss F, Traisnel M, Lagrenee M (2001) Influence of 2,5-bis(4-dimethylaminophenyl)-1,3,4-thiadiazole on corrosion inhibition of mild steel in acidic media. J Appl Electrochem 31:41–48
52. Sastri VS, Perumareddi JR (1997) Molecular orbital theoretical studies of some organic corrosion inhibitors. Corrosion 53: 617–622
53. Lukovits I, Kalman E, Zucchi F (2001) Corrosion inhibitors—correlation between electronic structure and efficiency. Corrosion 57:3–8
54. Chao CY, Lin LF, Macdonald DD (1981) A point defect model for anodic passive films. J Electrochem Soc 128:1187–1194
55. Ritchie IM, Bailey S, Woods R (1999) The metal–solution interface. Adv Colloid Interface Sci 80:183–231
56. Mu GN, Zhao TP, Liu M, Gu T (1996) Effect of metallic cations on corrosion inhibition of an anionic surfactant for mild steel. Corrosion 52:853–856
57. Ahamad I, Quraishi MA (2010) Mebendazole: new and efficient corrosion inhibitor for mild steel in acid medium. Corros Sci 52:651–656